INT. COMM. HEAT MASS TRANSFER
Vol. 18, pp. 779-789, 1991

0735-1933/91 $3.00 + .00
Printed in the United States

THERMAL PERFORMANCE OF AN AMMONIA-WATER REFRIGERATION SYSTEM

Jose A. Manrique
Instituto Tecnologico y de Estudios Superiores de Monterrey
Department of Thermal Engineering
Monterrey, N. L., Mexico

(Communicated by J.P. Hartnett and W.J. Minkowycz)

ABSTRACT

The conservation and efficient use of energy has led to alternate methods for air conditioning in buildings. Presently, two types of absorption air conditioning systems are widely used: the lithium-bromide-water system and the ammonia-water system. The first type is typically a water fired absorption chiller while the second one is a gas fired chiller. Some of the lithium-bromide-water systems use as a source of heat a stream of hot water supplied from solar collectors at a temperature level of the order of 95-100 °C. The purpose of this paper is to explore the possibilities to use solar energy to operate an ammonia-water system and to predict its thermodynamic performance.

The results indicate that it is feasible to use solar energy to operate an ammonia-water absorption-refrigeration system.

Introduction

The conservation and efficient use of energy has led to alternate methods for air conditioning in buildings. Presently, two types of absorption air conditioning systems are widely used: the lithium-bromide-water system and the ammonia-water system. The first type is typically a water fired absorption chiller while the second one is a gas fired chiller. Some of the lithium-bromide-water systems use as a source of heat a stream of hot water supplied from solar collectors at a temperature level of the order of 95-100 °C. Several authors have studied its performance in detail [1-7]. The purpose of this paper is to explore the possibilities to use solar energy to operate an ammonia-water system and to predict its thermodynamic performance.

The gas fired unit under consideration operates on an ammonia-water (ammonium hydroxide - NH4OH) absorption-refrigeration cycle. Ammonia is the refrigerant and distilled water is the absorbent. In this case water has a very high affinity for the refrigerant vapor. A

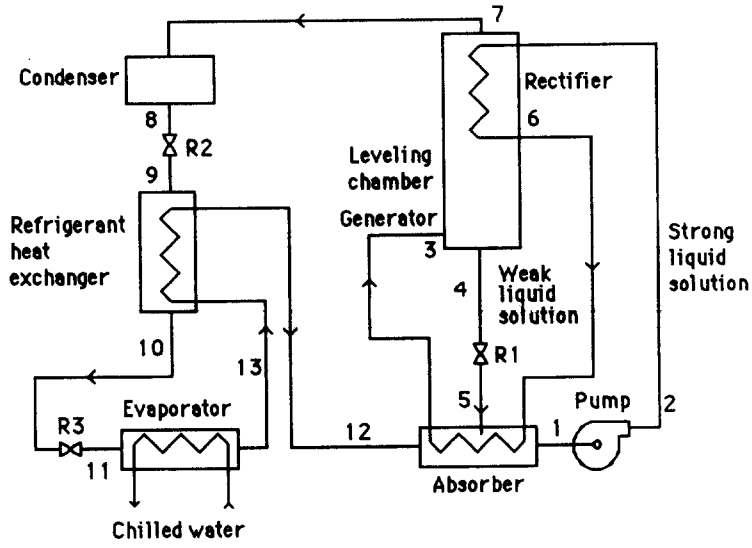

FIG. 1

Schematic diagram of an ammonia-water absorption-refrigeration system.

schematic diagram of the system is shown in Figure 1.

Operating pressures are primarily controlled by the temperature of the ambient air drawn across the air cooled condenser-absorber section. Pressure separations are maintained during operation by restrictors in both the refrigerant and solution lines and a check valve on either side of the solution pump.

On cooling demand from an external control, heat from the gas burner is applied to the generator, causing the solution inside to boil. Since the refrigerant vaporizes at a much lower temperature than water, a high percentage of the refrigerant vapor and a small amount of water vapor rises to the top of the generator. For example, at an arbitrary saturation pressure of 2000 kPa the ammonia boils at 49.6 °C while water boils at 212.4 °C. The remaining solution (weak solution) tends to gravitate to the bottom of the generator. As this boiling action takes place, the high side pressure is increased. This pressure forces the weak solution through a strainer and restrictor (R1) where it is reduced to the low side pressure,

and the weak solution is then metered into the solution cooled absorber (State 5).

Referring again to the diagram of Figure 1, the refrigerant vapor rises to the top of the generator. This vapor leaves the generator and enters a leveling chamber. The leveling chamber is designed to slow down the flow of vapor causing it to drop some of the water wich is carried from the generator. Leaving the leveling chamber, the vapor now passes into the rectifier. This is simply a heat exchanger. Inside the rectifier is a coil through which strong solution is flowing to the generator. This solution is cooler than the vapor passing across it. When the hot vapor makes contact with the cooler coil it will condense any water vapor which it has carried from the generator and the leveling chamber. This weak solution drains to the bottom of the rectifier and returns through the condensate line to the generator.

Refrigerant vapor leaves the rectifier at high pressure and temperature. This vapor (State 7) enters the condenser coils. The condenser fan is moving ambient air across the outside of these coils; which removes heat from the refrigerant vapor causing a change of state from vapor to liquid. The liquid refrigerant passes from the condenser through the first two refrigerant strainer restrictor assemblies (R2) into the refrigerant heat exchanger. As the liquid refrigerant moves through the outer chamber of the heat exchanger, it is further cooled (State 10). The liquid refrigerant then passes through a second refrigerant strainer restrictor assembly (R3), where it is reduced to the low side pressure as it enters the evaporator (State 11). Flowing over the outside of the evaporator coil is water cotaining energy removed from the conditioned space. Heat from this water causes the refrigerant to boil at a low temperature. As the water gives up heat to the refrigerant, this vaporizes and the water is chilled to be recirculated to the conditioned space.

The refrigerant vapor leaves the evaporator and enters the inner section of the refrigerant heat exchanger (State 13). Here it picks up heat from the liquid refrigerant moving counterflow in the outer section of the refrigerant heat exchanger. The vapor then enters the solution cooled absorber (State 12) where it is reunited with the weak solution (State 5). The strong solution leaves the absorber and enters the inlet tank of the solution pump (State 1). This is a volume displacement pump utilizing an inlet check valve, a discharge check valve and a diaphragm operated in conjunction with a hydraulic pump designed to deliver a pulsating manometric pressure from 0 to 2750 kPa approximately. As the strong solution leaves the solution pump it enters the inside coil of the rectifier (State 2), where it removes heat from the hot vapor being passed across the coil. The strong solution enters the inside coil of the solution cooled absorber (State 6) where additional heat is gained from weak solution being distributed over the outside of this coil. With the preheated strong solution returning to the generator (State 3) the cycle is completed.

Thermodynamic Analysis

A 5 ton gas fired chiller and its air handler were installed in an experimental house at the Solar Energy Laboratory. Several thermocouples were adhered for temperature measurements. The building has a maximum computed cooling load of 16767 W (4.8 ton.) This load was calculated by using the E20-II computer program developed by Carrier [7].

The HYSIM [8] simulation program was used to carry out the thermodynamic analysis of the system. Figure 2 depicts the equilibrium temperature as a function of ammonia mass fraction at a constant saturation pressure by using the Peng-Robinson equation of state, activity models, and data obtained by ASHRAE charts [9]. The Peng-Robinson equation of state was chosen since it is reliable over a wide range of conditions.

Several assumptions were made in the analysis to fix the operating concentrations and pressures in the cycle. Some of them were based on experimental results:

i. The liquid refrigerant temperature at the air cooled condenser outlet is basically equal to the ambient temperature plus 10 °C, i.e.,

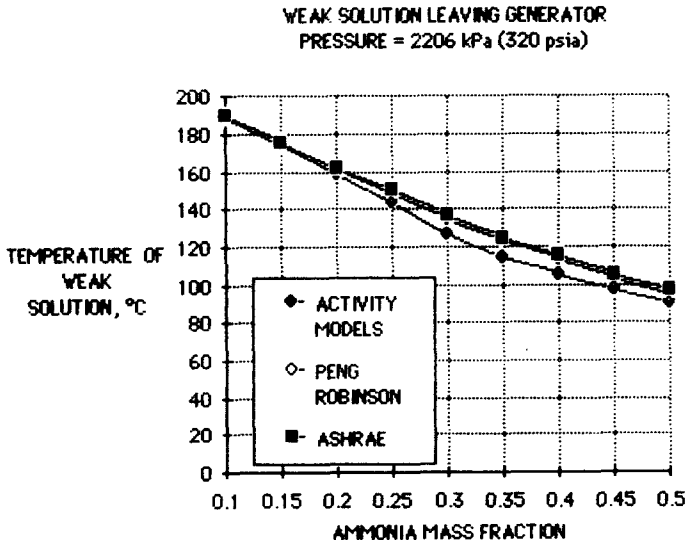

FIG. 2

Liquid temperature as a function of ammonia mass fraction at a constant pressure.

$$T_8 = T_{amb} + 10 \quad (1)$$

An ammonia mass fraction concentration of about 0.998 is assumed here. This information defines the high side equilibrium pressure in the cycle.

ii. The temperature of the weak solution leaving the generator obeys the following experimental linear relationship in the range of ambient temperatures analyzed,

$$T_4 = 0.83T_{amb} + 89.83 \quad (2)$$

Since thermodynamic State 4 has the same high pressure as point 8, the ammonia concentration of State 4 is found. Furthermore, $x_4 = x_5$.

iii. The strong liquid solution concentration is fixed by using the following relationship for equilibrium State 3,

$$T_3 = 0.83\ T_{amb} + 81.83 \quad (3)$$

Since thermodynamic State 3 is assumed to be at the same high pressure in the cycle, the ammonia concentration of states 1, 2, 6 and 3 are found. Notice that there is a temperature difference of 8 °C between states 3 and 4.

iv. The gas fired unit under consideration has the air cooled absorber and condenser near each other. However, the temperature of State 1 follows the relationship,

$$T_1 = T_{amb} + 8 \quad (4)$$

Since the ammonia mass fraction of State 1 is already known, the low side pressure of the cycle can be computed with this information.

v. The temperature of State 9 is of the order of 32 °C. This value and its concentration fix the intermediate pressure in the cycle.

Other assumptions for the thermodynamic cycle are:

I. The temperature increase of the strong solution in the rectifier is of the order of 20 °C, i.e., $T_6 = T_{amb} + 28$.

II. The temperature of refrigerant is reduced 18 °C in the heat exchanger.

III. Equilibrium (saturated) conditions for States 1, 3, 4, 7, 8, and 12 are assumed.

IV. The pump mechanical efficiency is assumed to be 75 percent.

It might appear that the ammonia mass fraction of 0.998 for State 8 was somewhat arbitrary. However, consider the following data for an ambient temperature of 33 °C. Figure 3 shows the equilibrium temperature of State 12 (vapor) for different concentrations and a constant pressure of 303.3 kPa. Similarly, it shows the equilibrium temperature of high pressure vapor as a function of ammonia concentration in State 7 when the saturated liquid is at 43 °C. Notice that the high pressure vapor temperature (T_7) must be above the outlet condenser-absorber air temperature, which is approximately 50 °C in this case; and the low pressure vapor temperature (T_{12}) must be below T_9 = 32 °C as seen from the heat exchanger of Figure 1. Thus, from Figure 3 it is observed that the ammonia mass traction for states 8, 9, ..., 13 must be 0.998, approximately. Furhermore, notice that the saturation temperatures of pure ammonia are 43 °C and -8.6 °C for the high and low pressures, respectively.

Results and Discussion

Figure 4 shows different operating temperatures which were measured in the chiller. The numbers correspond to those states shown in Figure 1. It is observed that the highest temperature in the cycle is of the order of 120 °C.

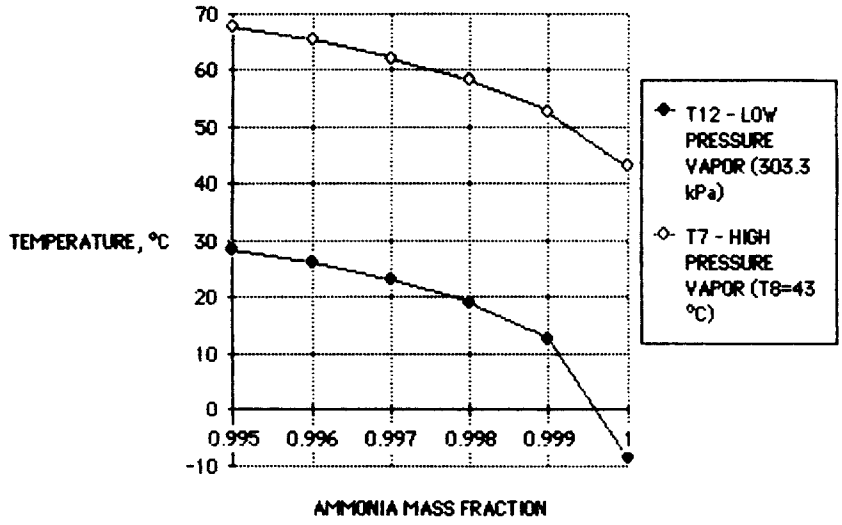

FIG. 3

Vapor temperature as a function of ammonia mass fraction.

Energy and mass balances were carried out in every individual process of the cycle. The mass flow rates in the cycle were calculated by using the following relationships:

$$m_8 = m_{12} = Q_{ev} / (h_{12} - h_8) \quad (5)$$

$$m_{12} + m_5 = m_1 \quad (6)$$

$$m_{12}x_{12} + m_5x_5 = m_1x_1 \quad (7)$$

Thus,

$$m_5 = m_{12}(x_{12} - x_1)/(x_1 - x_5) \quad (8)$$

The thermodynamic cycle was simulated as shown in Figure 5. The computed temperatures shown here correspond to an ambient temperature of 33 °C. The system produces 5 tons of refrigeration. It is observed that the highest temperature in the generator is 118 °C, while the lowest temperature of -9 °C occurs in the refrigerant at the evaporator inlet. Neglecting the pump power it is found that the coefficient of performance is 0.33 for

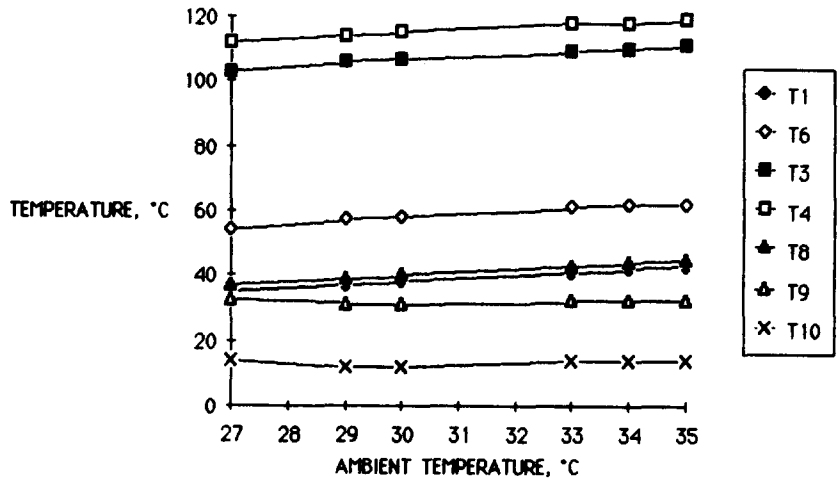

FIG. 4

Experimental temperatures in a 5 ton ammonia-water refrigeration system.

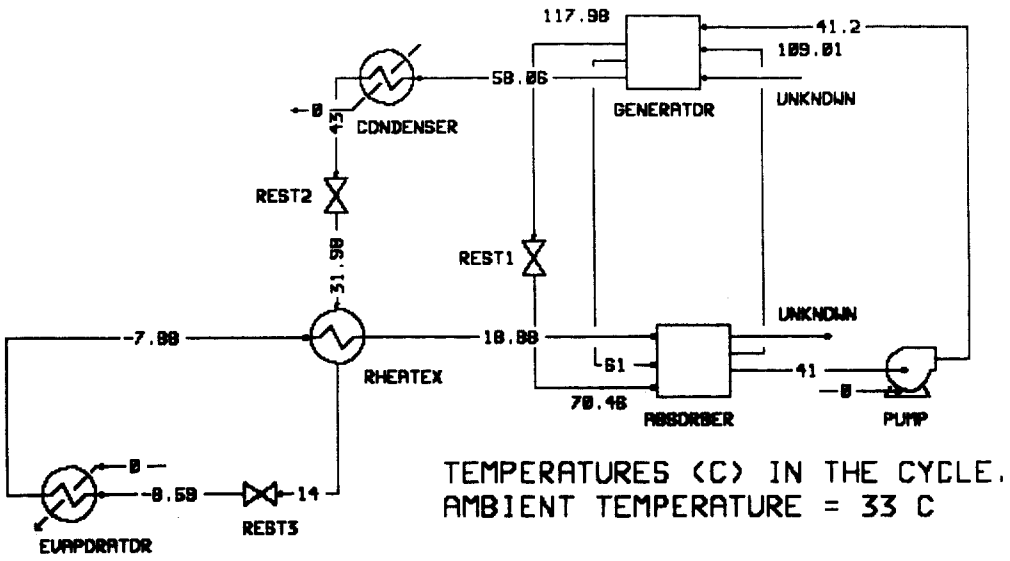

FIG. 5

Computed temperatures in the thermodynamic cycle.

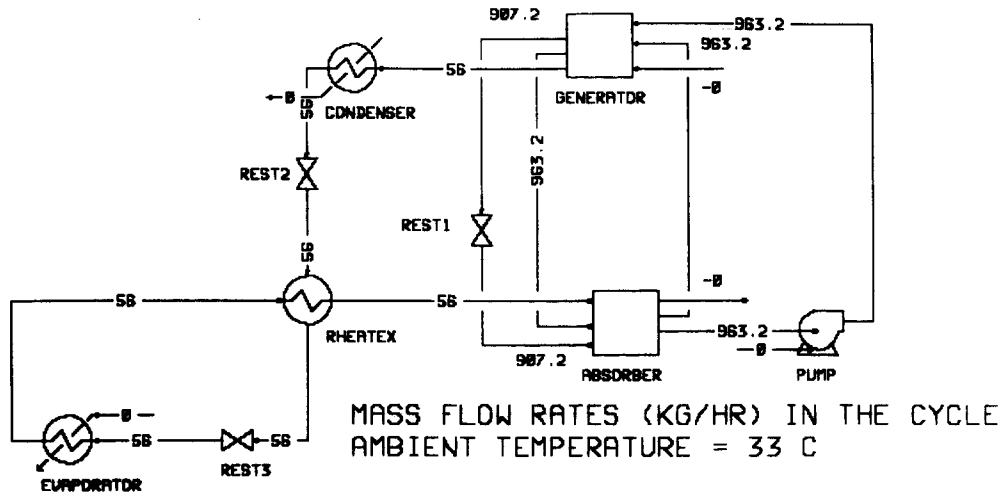

FIG. 6

Computed mass flow rates in the thermodynamic cycle.

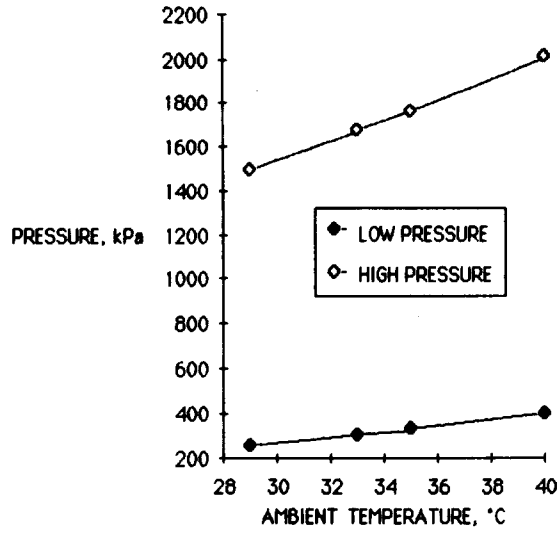

FIG. 7

Operating pressures in the ammonia-water refrigeration-absorption system.

these conditions. Similarly, Figure 6 shows different mass flow rates throughout the system for the same value of ambient temperature.

Figure 7 shows different computed absolute pressures in the chiller for various values of ambient temperature.

Figure 8 shows energy flow rates in the system. It is noticed that the pump work is very small, as it was expected. On the other hand, the evaporator load decreases slightly as the ambient temperature increases. At 33 °C the generator requieres 52510 W of heat, and the total heat rejected -absorber plus condenser- is 52469 + 18223 = 70692 W.

Conclusions

The agreement between computed and experimental temperatures in the cycle was very satisfactory. The coefficient of performance of a system may be improved by using in the design process an analysis similar to the one described in this paper.

It can be concluded that the ammonia-water absorption system can operate with solar energy and a synthetic heat transfer fluid. From the above results it is observed that the

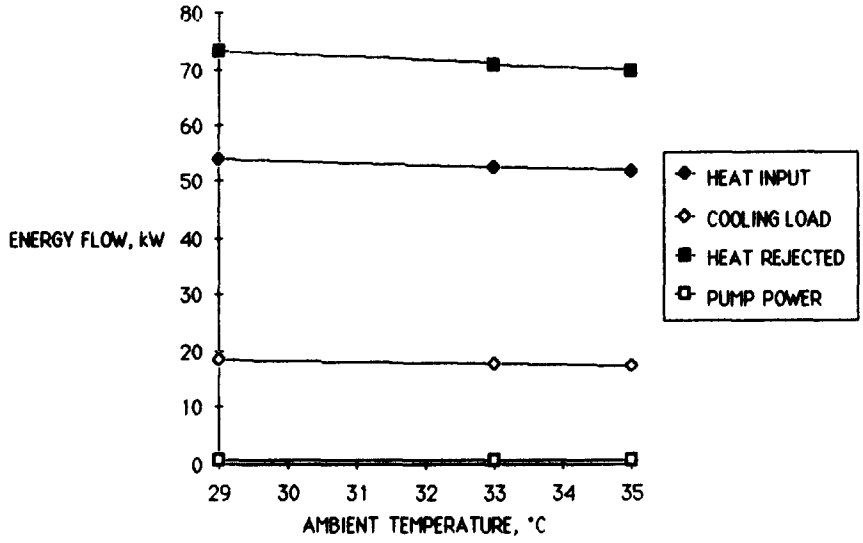

FIG. 8

Energy balance in a 5 ton ammonia-water refrigeration-absorption chiller.

highest temperatures in the cycle are of the order of 120 °C. Therefore, with the use of compound parabolic concentrators, evacuated heat pipes or focusing concentrators these temperatures can be achieved with a reasonable efficiency.

Some of the compound parabolic concentrators which have been evaluated at the Solar Enery Laboratory [10] with a concentration ratio of 1.6 exhibited an efficiency of 45 percent for an inlet temperature of 142 °C and a total solar radiation of 780 W/m^2. The optical efficiency of these fixed concentrators is of the order of 52 percent.

Nomenclature

m	mass flow rate
Q	heat flow
x	ammonia mass fraction
T	temperature

Subscripts

amb ambient

1,2,3,...

thermodynamic state

References

1. M. Dalichaouch, Energy analysis of absorption-refrigeration cycles, Journal of the Institute of Energy, 63, p. 167, (1990).

2. M. J. P. Bogart, Lithium Bromide Absorption Refrigeration - A Calculator Program, ASHRAE Journal, 24, 8, p. 23, (1982).

3. J. F. Kreider and F. Kreith, Solar Heating and Cooling: Engineering, Practical Design, and Economics, McGraw-Hill, p. 161, (1977).

4. José A. Manrique, Diseño y Construcción de una Casa Solar, Ciencia Interamericana, 21, 1-4, p. 9, (1981).

5. James L. Threlkeld, *Thermal Environmental Engineering*, Prentice-Hall, Inc., p. 85, (1971).

6. W. F. Stoecker and J. W. Jones, *Refrigeration and Air Conditioning*, McGraw-Hill, p. 328, (1982).

7. Carrier Software Systems, E20-II, Carrier Corporation, (1987).

8. HYSIM, Hyprotech Ltd., Houston, TX, (1987).

9. ASHRAE *Handbook of Fundamentals*, American Society of Heating, Refrigerating and Air-Conditioning Engineers, Inc., Atlanta, GA, p. 17.68, (1989).

10. Jose A. Manrique, A Compound Parabolic Concentrator, Int. Comm. Heat Mass Transfer, 11, 3, p. 267, (1984).